

# STREAK CAMERA MEASUREMENT OF ELECTRON BEAM ENERGY LOSS PER TURN IN THE ADVANCED PHOTON SOURCE PARTICLE ACCUMULATOR RING\*

K. P. Wootton<sup>†</sup>, J. R. Calvey, J. C. Dooling, K. C. Harkay, Y. Sun, B. X. Yang  
Argonne National Laboratory, Lemont, IL 60439, USA  
A. H. Lumpkin, Argonne Associate of Global Empire, LLC,  
Argonne National Laboratory, Lemont, IL 60439, USA

## Abstract

Relativistic electron beams in storage rings radiate a significant fraction of beam energy per turn. As demonstrated in previous experiments, with the radiofrequency accelerating structures off, the turn-by-turn time of arrival of the electron bunch can be observed from the synchrotron radiation that it produces using a streak camera. In the present work, we present measurements of the energy loss per turn of an initially short electron bunch (~1 ps RMS) from a photocathode electron gun in the Advanced Photon Source Particle Accumulator Ring (375 MeV, 102 ns revolution period). With the streak camera synchroscan locked to the twelfth harmonic of the revolution frequency (117.3 MHz), we observe an injection transient in the horizontal direction.

## INTRODUCTION

Injecting and accumulating charge in an electron storage ring is a dynamic process. It relies upon the emission of incoherent synchrotron radiation to damp the beam phase space to an equilibrium distribution. The energy loss per turn due to incoherent synchrotron radiation has previously been observed at GeV-scale electron storage rings [1, 2]. In those experiments, the electron beam was injected into the storage ring with the radiofrequency (RF) cavities switched off.

In the present work, dual-sweep streak camera measurements were performed which uniquely show inherent energy spread effects on the bunch length per turn, electron beam energy loss per turn, and the injection transverse transient for the initial ~1 ps duration bunch injected at 375 MeV.

## THEORY

### Energy Loss per Turn

In the absence of an accelerating RF voltage, an electron loses energy  $U_0$  each turn due to incoherent synchrotron radiation [3]. The energy loss per turn can be calculated using the second synchrotron radiation integral  $I_0$  [4]. Due to the non-zero momentum compaction factor  $\alpha_c$  of the ring [4], the electron follows a dispersive orbit and arrives earlier each turn. At a time  $t$  following injection, the

change in arrival time of the electron bunch relative to the synchronous arrival time is given by [1]:

$$\Delta T_{\text{tot}} = \frac{1}{2} \frac{f_0}{E} \alpha_c U_0 t^2, \quad (1)$$

where  $f_0$  is the revolution frequency, and  $E$  is the electron beam energy.

### Injection Transient

Injection transients have previously been observed using turn-by-turn optical measurements at other laboratories [5–10]. For beams injected transversely off-axis for accumulation in a storage ring, the beam centroid is observed to oscillate at the betatron frequency in the plane of the orbit offset. In the Particle Accumulator Ring (PAR), electrons are injected with a horizontal offset from the central beam axis.

Beam centroid oscillations are observed at the betatron frequency if there is a dispersion mismatch, and oscillate at twice the betatron frequency if there is a beta function mismatch [11]. The observation of such transverse effects are deducible from dual-sweep streak camera images.

## METHOD

A chain of injectors is used to accelerate electrons at the Advanced Photon Source (APS). The injector chain is illustrated schematically in Fig. 1 [12]. In the present work, we utilise electron beams from the photocathode gun (PCG) [13] and RF thermionic gun 2 (RG2) [14]. These beams are accelerated using the main linac accelerating structures (L2, L4 and L5), and injected into the PAR.

The PAR is operated as an electron damping ring [15]. In normal operation, beams injected from the linac are accumulated over multiple linac cycles and damped before injection as a single bunch into the booster synchrotron. The PAR RF system features two cavities with the fundamental RF cavity operating at the revolution frequency 9.77 MHz, and a 12<sup>th</sup> harmonic bunch compressing cavity operating at 117.2 MHz [16]. Calculated parameters of the PAR are summarised in Table 1.

To observe the electron beam arrival on a turn-by-turn basis, we used a streak camera installed at the PAR West synchrotron light port: a location in the lattice with non-zero horizontal dispersion [17–19]. The Hamamatsu model C5680 streak camera was operated in the dual-sweep configuration. A synchroscan module was used as the deflector

\* Work supported by the U.S. Department of Energy, Office of Science, Office of Basic Energy Sciences, under Contract No. DE-AC02-06CH11357.

<sup>†</sup> kwootton@anl.gov

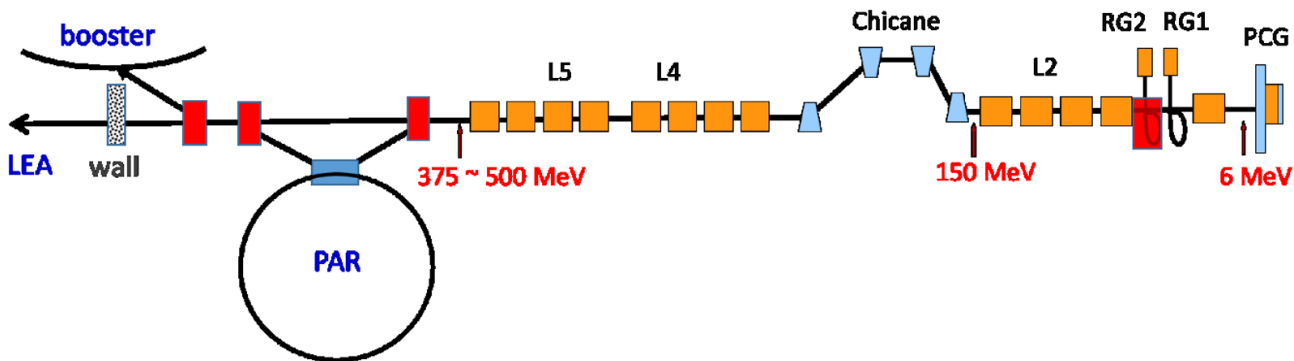


Figure 1: Schematic layout of the APS linac and PAR injector chain. In the present work, we utilise electron beams from the photocathode gun (PCG) and RF thermionic gun 2 (RG2). These beams are accelerated using the main linac accelerating structures (L2, L4 and L5), and injected into the Particle Accumulator Ring (PAR) at 375 MeV. (Reproduced under Creative Commons license CC-BY 4.0 from [S. Shin *et al.*, *Phys. Rev. Accel. Beams*, vol. 21, p. 060101, 2018], Ref. [12])

Table 1: PAR Parameters for the Present Experiment

| Parameter                             | Symbol     | Value | Units           |
|---------------------------------------|------------|-------|-----------------|
| Beam energy                           | $E$        | 0.375 | GeV             |
| Revolution period                     | $T$        | 102   | ns              |
| Betatron tune ( $x$ )                 | $\nu_x$    | 2.177 | –               |
| Betatron tune ( $y$ )                 | $\nu_y$    | 1.211 | –               |
| Momentum compaction factor            | $\alpha_c$ | 0.244 | –               |
| Second synchrotron radiation integral | $I_2$      | 6.16  | $\text{m}^{-1}$ |
| Energy loss per turn                  | $U_0$      | 1.72  | keV             |

in the vertical plane (synchronised with the 117.1 MHz RF signal), on sweep range 4 (1.48 ns full scale, 3.0 ps per pixel). A slow dual axis unit was used as the horizontal deflector, varying the sweep range between 1-10  $\mu\text{s}$  (10-100 turns of the PAR).

## RESULTS

### Stored Beam at Equilibrium

The longitudinal profile of the electron beam over several turns at equilibrium with both the fundamental and the 12<sup>th</sup> harmonic RF cavities powered [15] is plotted in Fig. 2.

From Fig. 2, we confirmed that the damped electron bunches arrive at an equal revolution period of 102 ns, and we validated the horizontal time axis calibration. The equilibrium bunch length was determined to be  $\sim 300$  ps from the vertical axis image signal distribution.

### Photocathode Gun Beam

To observe longitudinal electron beam dynamics at injection, we accelerate a single  $\sim 1$  ps electron bunch from the photocathode gun using the linac, and inject it into the PAR. This is illustrated in Fig. 3 over the first 1  $\mu\text{s}$  following injection (the first  $\sim 8$  turns), and Fig. 4 over a timescale of the first 2  $\mu\text{s}$  following injection (the first  $\sim 16$  turns).

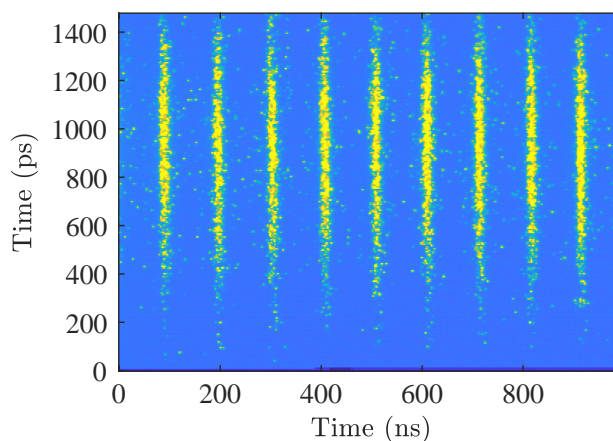


Figure 2: Observation over 9 turns of the PAR of a single electron bunch stored beam at equilibrium, with both the fundamental and 12<sup>th</sup> harmonic RF cavity on.

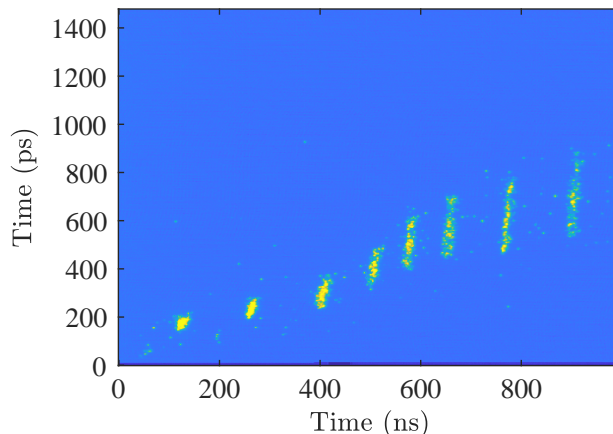


Figure 3: Observation over the first eight turns of a single electron bunch from the photocathode RF gun injected into the PAR. The slow streak range (horizontal axis) of the streak camera was 1  $\mu\text{s}$ . Both the fundamental and 12<sup>th</sup> harmonic RF cavity were off.

Content from this work may be used under the terms of the CC BY 3.0 licence (© 2020). Any distribution of this work must maintain attribution to the author(s), title of the work, publisher, and DOI

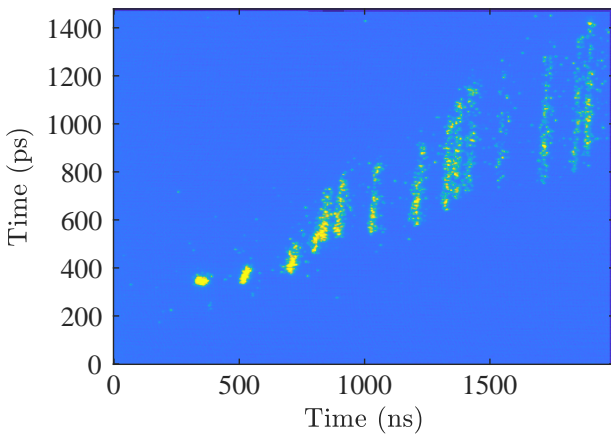


Figure 4: Observation over the first sixteen turns of a single electron bunch from the photocathode RF gun injected into the PAR. The slow streak range (horizontal axis) of the streak camera was  $2\ \mu\text{s}$ . Both the fundamental and 12<sup>th</sup> harmonic RF cavity were off.

### Thermionic Gun Beam

Another option for injecting into the linac is to use the RF thermionic guns. We accelerated a  $\sim 10\ \text{ns}$  duration electron bunch train from RF thermionic gun 2 gun using the linac [14], and injected it into the PAR. This is illustrated in Fig. 5 over the first  $1\ \mu\text{s}$  following injection.

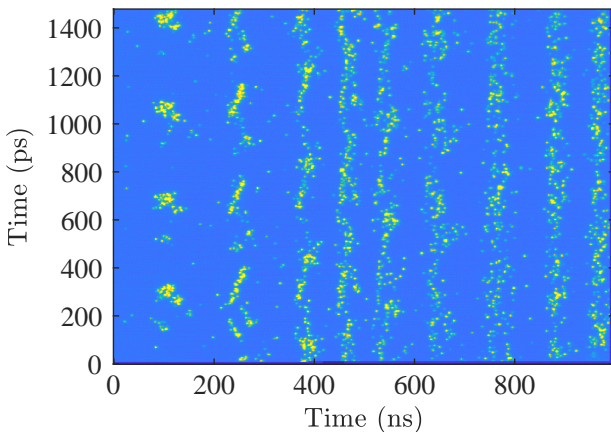


Figure 5: Observation over the first nine turns of a  $\sim 12\ \text{ns}$  duration electron bunch train from the thermionic RF gun injected into the PAR. Electron bunches in the train are separated along the vertical axis by  $350\ \text{ps}$  corresponding to the RF frequency of the electron gun ( $2856\ \text{MHz}$ ). Both the fundamental and 12<sup>th</sup> harmonic RF cavity were off.

## DISCUSSION

Since the streak camera horizontal axis has both spatial and slow temporal information, the transverse injection transient results in the shift of the peak positions away from the regular temporal spacings along the slow (horizontal) time axis of Fig. 2. This means that in principle the amplitude of

the horizontal oscillation could be extracted from the images with further analysis.

Unlike in Fig. 2, for the injected beam in Figs. 3–4, it appears that the beam arrival time observed on the horizontal (slow) axis of the streak camera is oscillating in time, with a period of about six turns. Based on the period of oscillation corresponding approximately with the fractional horizontal betatron period, we associate this oscillation with a mismatched horizontal injection transient, rather than a temporal oscillation. Another possible mechanism to consider is the effect of coherent synchrotron radiation in the THz frequency scale on the energy loss per turn.

Parabolic fits for the energy loss per turn are presented in Fig. 6, bounding the time of arrival of the electron beam envelope in time. One possibility for the discrepancy between the observed and calculated energy loss per turn could be a mismatch of the beam energy with the ring at injection [2].

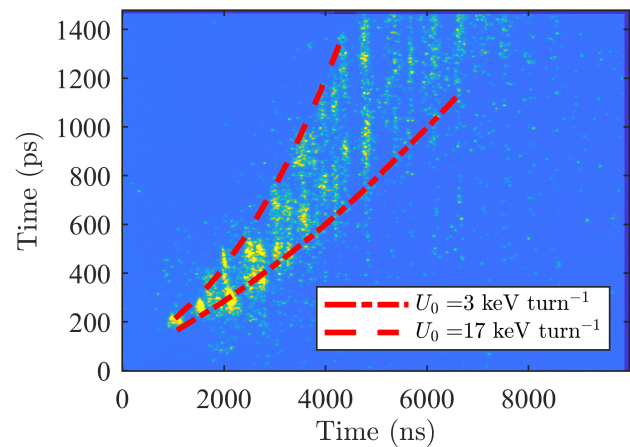


Figure 6: Observation over the first turns of a single electron bunch from the photocathode RF gun injected into the PAR. The slow streak range (horizontal axis) of the streak camera was  $10\ \mu\text{s}$ . Both the fundamental and 12<sup>th</sup> harmonic RF cavity were off. Parabolic fits for the maximum and minimum energy loss per turn observed are plotted.

## CONCLUSION

Using a streak camera, we have observed the time of arrival and bunch lengthening of a  $\sim 1\ \text{ps}$  electron bunch for the turns immediately following injection into the PAR electron damping ring. With the streak camera synchroscan unit locked to the twelfth harmonic of the revolution frequency ( $117.3\ \text{MHz}$ ), we observe an injection transient in the horizontal direction. An energy loss per turn of the electron beam was observed to be  $3\ \text{keV turn}^{-1} < U_0 < 17\ \text{keV turn}^{-1}$  compared to the model of  $U_0 = 1.7\ \text{keV turn}^{-1}$ .

## ACKNOWLEDGEMENTS

The submitted manuscript has been created by UChicago Argonne, LLC, Operator of Argonne National Laboratory (“Argonne”). Argonne, a U.S. Department of Energy Office of Science Laboratory, is operated under Contract No.

DE-AC02-06CH11357. The U.S. Government retains for itself, and others acting on its behalf, a paid-up nonexclusive, irrevocable worldwide license in said article to reproduce, prepare derivative works, distribute copies to the public, and perform publicly and display publicly, by or on behalf of the Government. The Department of Energy will provide public access to these results of federally sponsored research in accordance with the DOE Public Access Plan.

<http://energy.gov/downloads/doe-public-access-plan>

## REFERENCES

- [1] J. M. Byrd and S. De Santis, “Longitudinal injection transients in an electron storage ring”, *Phys. Rev. ST Accel. Beams*, vol. 4, p. 024401, 2001.  
doi:10.1103/PhysRevSTAB.4.024401
- [2] A. A. Nosych, B. Bravo, and U. Iriso, “Energy Loss Measurements with Streak Camera at ALBA”, in *Proc. 7th Int. Beam Instrumentation Conf. (IBIC’18)*, Shanghai, China, Sep. 2018, pp. 548–551.  
doi:10.18429/JACoW-IBIC2018-THOB02
- [3] J. Schwinger, “On the Classical Radiation of Accelerated Electrons”, *Phys. Rev.*, vol. 75, pp. 1912–1925, 1949.  
doi:10.1103/PhysRev.75.1912
- [4] R. H. Helm, M. J. Lee, P. L. Morton, and M. Sands, “Evaluation of Synchrotron Radiation Integrals”, *IEEE Trans. Nucl. Sci.*, vol. 20, pp. 900–901, 1973.  
doi:10.1109/TNS.1973.4327284
- [5] J. C. Bergstrom and J. M. Vogt, “The optical diagnostic beamline at the Canadian Light Source”, *Nucl. Instrum. Methods Phys. Res. Sect. A*, vol. 562, pp. 495–512, 2006.  
doi:10.1016/j.nima.2006.02.200
- [6] A. S. Fisher, M. Petree, R. Kraus, Y.-S. Au, and B. Chan, “Turn-by-Turn Imaging of the Transverse Beam Profile in PEP-II”, *AIP Conf. Proc.*, vol. 868, pp. 303–312, 2006.  
doi:10.1063/1.2401418
- [7] W. X. Cheng *et al.*, “Fast-Gated Camera Measurements in SPEAR3”, in *Proc. 23rd Particle Accelerator Conf. (PAC’09)*, Vancouver, Canada, May 2009, paper TH6REP032, pp. 4015–4017.
- [8] W. J. Corbett, W. X. Cheng, A. S. Fisher, and W. Y. Mok, “Injection Beam Dynamics in SPEAR3”, in *Proc. 14th Beam Instrumentation Workshop (BIW’10)*, Santa Fe, NM, USA, May 2010, paper TUPSM065, pp. 318–322.
- [9] J. Corbett, W. Cheng, A. S. Fisher, W. Mok, and S. Westerman, “Visible Light Diagnostics at SPEAR3”, *AIP Conf. Proc.*, vol. 1234, pp. 637–640, 2010.  
doi:10.1063/1.3463286
- [10] M. J. Boland, T. M. Mitsuhashi, and K. P. Wootton, “Turn-by-turn Observation of the Injected Beam Profile at the Australian Synchrotron Storage Ring”, in *Proc. 1st Int. Beam Instrumentation Conf. (IBIC’12)*, Tsukuba, Japan, Oct. 2012, paper MOPB83, pp. 276–278.
- [11] M. G. Minty and W. L. Spence, “Injection Envelope Matching in Storage Rings”, in *Proc. 16th Particle Accelerator Conf. (PAC’95)*, Dallas, TX, USA, May 1995, paper RAA06, pp. 536–538. doi:10.1109/PAC.1995.504711
- [12] S. Shin, Y. Sun, J. Dooling, M. Borland, and A. Zholents, “Interleaving lattice for the Argonne Advanced Photon Source linac”, *Phys. Rev. Accel. Beams*, vol. 21, p. 060101, 2018.  
doi:10.1103/PhysRevAccelBeams.21.060101
- [13] Y.-E. Sun *et al.*, “Commissioning of the Photo-Cathode RF Gun at APS”, in *Proc. 36th Int. Free Electron Laser Conf. (FEL’14)*, Basel, Switzerland, Aug. 2014, paper THP039, pp. 803–806.
- [14] J. W. Lewellen *et al.*, “Operation of the APS RF Gun”, in *Proc. 19th Int. Linac Conf. (LINAC’98)*, Chicago, IL, USA, Aug. 1998, paper TH4042, pp. 863–865.
- [15] E. A. Crosbie, “A Positron Accumulator Ring for APS”, Argonne National Laboratory, Argonne, IL, USA, Rep. LS-109, Mar. 1988. doi:10.2172/900005
- [16] Y. W. Kang, A. Nassiri, J. F. Bridges, T. L. Smith, and J. J. Song, “RF Cavities for the Positron Accumulator Ring (PAR) of the Advanced Photon Source (APS)”, in *Proc. 16th Particle Accelerator Conf. (PAC’95)*, Dallas, TX, USA, May 1995, paper WPP16, pp. 1693–1695.  
doi:10.1109/PAC.1995.505330
- [17] A. H. Lumpkin, “Advanced, time-resolved imaging techniques for electron-beam characterizations”, *AIP Conf. Proc.*, vol. 229, pp. 151–179, 1991. doi:10.1063/1.40746
- [18] A. Lumpkin and B. Yang, “Status of the synchrotron radiation monitors for the APS facility rings”, in *Proc. 16th Particle Accelerator Conf. (PAC’95)*, Dallas, TX, USA, May 1995, paper MPQ09, pp. 2470–2472.  
doi:10.1109/PAC.1995.505587
- [19] W. Berg, B. Yang, A. Lumpkin, and J. Jones, “Design and Commissioning of the Photon Monitors and Optical Transport Lines for the Advanced Photon Source Positron Accumulator Ring”, *AIP Conf. Proc.*, vol. 390, pp. 483–490, 1997.  
doi:10.1063/1.52325